PVP2006-ICPVT-11-93397

SUBSTITUTION OF HIGH-PRESSURE CHARGE BY ELECTROLYSIS CHARGE AND HYDROGEN ENVIRONMENT EMBRITTLEMENT SUSCEPTIBILITIES FOR INCONEL 625 AND SUS 316L

Kota Murakami*, Nobuaki Yabe*, Hiroshi Suzuki, Kenichi Takai**, Yukito Hagihara** and Yoru Wada*****

*Department of Mechanical Engineering, Graduate School of Science and Technology,
Sophia University, Tokyo 102-8554, Japan.
**Department of Mechanical Engineering, Faculty of Science and Technology, Sophia University, Tokyo, Japan.
***Japan Steel Works, Ltd., Muroran Research Laboratory, Hokkaido, Japan.

ABSTRACT

Hydrogen-fuel-cell vehicles have been developed and the gaseous pressure in the current major storage tanks of the vehicles varies from 35 to 70 MPa because of the demand for the increase in running distance. Hydrogen refueling stations are required to be resistant to 100 MPa hydrogen gas and the alloys used for such stations are required to have an excellent resistance to hydrogen environment embrittlement (HEE). The purposes of the present study are to substitute the high-pressure gaseous charge of hydrogen by electrolysis charge and to evaluate hydrogen degradation susceptibilities for Inconel 625 and SUS 316L in the environments substituted by electrolysis charge. Electrolysis hydrogen was charged to Inconel 625 and SUS 316L at various electrolysis fugacities and gaseous hydrogen was charged from 0.3 to 45 MPa hydrogen gas at 90 °C. Hydrogen states and contents were compared using thermal desorption analysis (TDA). Hydrogen degradation susceptibilities were evaluated using the slow strain rate technique (SSRT) at a constant extension rate of $8.6X10^{-6}$ /s at room temperature. The fundamental properties of thermal hydrogen desorption for Inconel 625 and SUS 316L were first analyzed to compare the hydrogen states after hydrogen charge by electrolysis and high pressure. The peak temperatures and profiles of hydrogen desorption do not change with charging temperature. When hydrogen is charged by electrolysis and high pressure until hydrogen saturation at 90 °C, the peak temperatures and profiles are the same in both environments. This means that hydrogen diffusion during and hydrogen states after hydrogen absorption are independent of charging method in spite of the differences in adsorption and dissociation reaction on the specimen surfaces. Using Sieverts law, the fugacity of electrolysis can transform into gaseous pressure. This indicates that high-pressure hydrogen environments in pipes or other components at hydrogen refueling stations can be substituted by electrolysis charge. Fracture strain in Inconel 625 decreases as hydrogen content charged by electrolysis increases, whereas that in SUS 316L does not change regardless of the hydrogen content of 161.5 mass ppm. Grain boundary fracture is observed on the surface of Inconel 625 absorbing a hydrogen content of 27.5 mass ppm, which corresponds to 59.2 MPa hydrogen gas at R.T using Sieverts law. In contrast, the fracture surfaces of SUS 316L hydrogen-charged at extremely high fugacities remain ductile dimples. Thus, hydrogen degradation susceptibility is much lower for SUS 316L than for Inconel 625.

1 INTRODUCTION

Hydrogen-fuel-cell vehicles have been developed because hydrogen and oxygen, which are used as fuel, are abundant and their reaction is clean. The gaseous pressure in the current major storage tanks of such vehicles varies from 35 to 70 MPa [1, 2] because of the demand for the increase in running distance. Furthermore, hydrogen refueling stations are required to be resistant to 100 MPa hydrogen gas. There are, however, a number of reports [3-5] that metals suffer from hydrogen environment embrittlement (HEE) when strained in a hydrogen gas environment. Therefore, the alloys used for hydrogen refueling stations are required to have an excellent resistance to HEE.

Actually, it is relatively difficult to actualize a high-pressure hydrogen gas environment due to cost and safety. Using easier and safer hydrogen-charging methods is preferable. The purposes of this study are to substitute the high-pressure gaseous charge by electrolysis charge and to evaluate hydrogen degradation susceptibilities for Inconel 625 and SUS 316L in the environments substituted by electrolysis charge.

2 EXPERIMENTAL

Inconel 625 and SUS 316L having a thickness of 0.2 mm and 0.25 mm were used in this study. The specimens were solution-treated. The chemical compositions, solution treatment conditions and mechanical properties are shown in Tables 1 and 2. Electrolysis hydrogen was charged in the electrolysis of H_2SO_4 with or without NH_4SCN under various current densities at 90 °C. Gaseous hydrogen was charged from 0.3 to 45 MPa at 90 °C. No damage was observed on the specimen surfaces when hydrogen was charged under the above charging conditions. Hydrogen states and contents were compared using thermal desorption analysis (TDA). Hydrogen degradation susceptibilities were evaluated using the slow strain rate technique (SSRT) at a constant extension rate of 8.6X 10^{-6} /s at room temperature.

Table1 Chemical Compositions of Inconel 625 and SUS 316L

	Chemical compositions (%)					
Specimens	Mn	Ni	Cr	Mo	Fe	Nb
Inconel 625	0.2	60.8	21.5	8.9	3.9	3.5
SUS 316L	0.7	12.1	17.1	2.8	Bal.	0.1

Table 2 Solution Treatment Conditions and Mechanical Properties of Inconel 625 and SUS 316L.

	Solution treatment	T. S. MPa
Inconel 625	1150℃X2h	700
SUS 316L	1100℃X3h	400

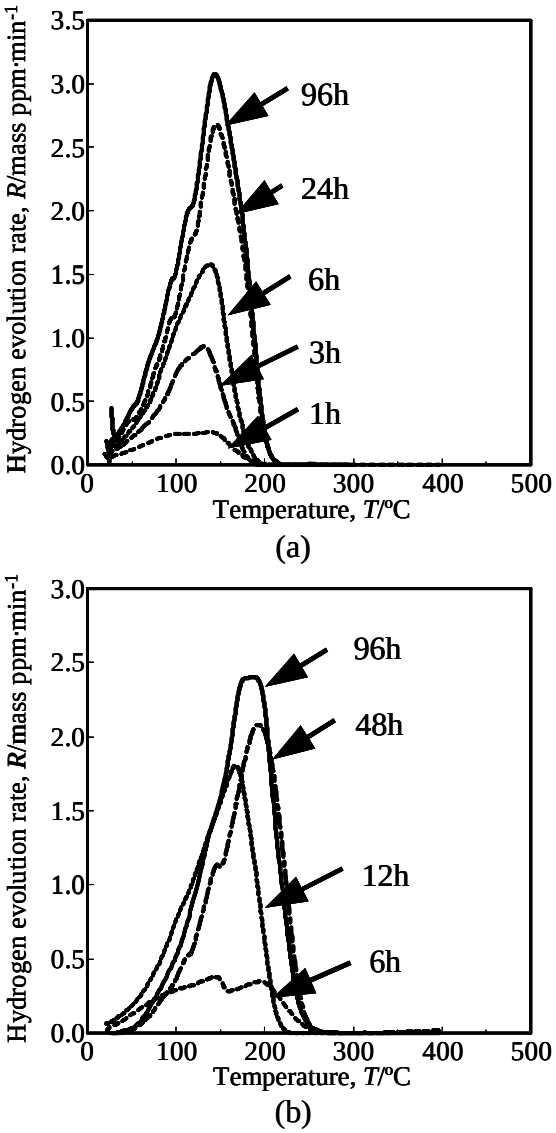

Fig. 1 Hydrogen Evolution Curves of (a) Inconel 625 and (b) SUS 316L at Various Hydrogen Charging Times by Electrolysis Charge

3 RESULTS

3.1 Fundamental Properties of Thermal Hydrogen Desorption

3.1.1 Effect of Hydrogen Charging Time Figures 1 (a) and (b), respectively, show hydrogen evolution curves of Inconel 625 and SUS 316L at various hydrogen charging times. The peak temperatures for Inconel 625 and SUS 316L are approximately 150 and 200 °C, respectively, and the hydrogen in the specimens is completely desorbed at approximately 300 °C. Fig. 2 shows the relationship between charging time and peak temperature. The peak temperatures shift to a higher temperature with increasing charging time and become constant. The hydrogen content in the specimens increases with charging time and becomes constant at almost the same time as the peak temperature, as shown in Fig. 3. Therefore, the peak temperatures for Inconel 625 and SUS 316L correspond to hydrogen diffusion from the surface to the center of the specimens.

3.1.2 Effect of Specimen Thickness Fig. 4 shows hydrogen evolution curves of Inconel 625 having various specimen thicknesses when hydrogen was charged until saturation. The peak temperature of the specimen with a thickness of 0.8 mm is approximately 400 °C. Hydrogen desorption at a higher temperature indicates detrap from deep traps and/or long diffusion of hydrogen in specimens. The peak temperatures shift to a lower temperature as the specimen thickness decreases from 0.8 to 0.1 mm. This suggests that the peak temperature shifts with specimen thickness and depends on hydrogen diffusion, not on trapping effects.

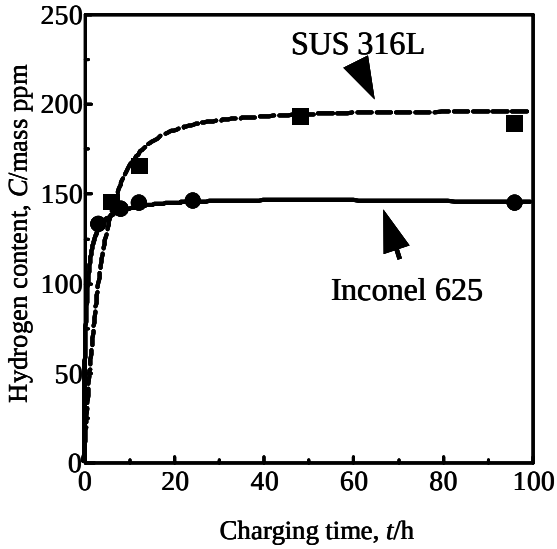

Fig. 3 The Relation between Charging Time and Hydrogen Content for Inconel 625 and SUS 316L when Hydrogen is Charged by Electrolysis

3.1.3 Effect of Charging Temperature Fig .5 (a) and (b) show hydrogen evolution curves of Inconel 625 and SUS 316L, respectively, under various charging temperatures in the

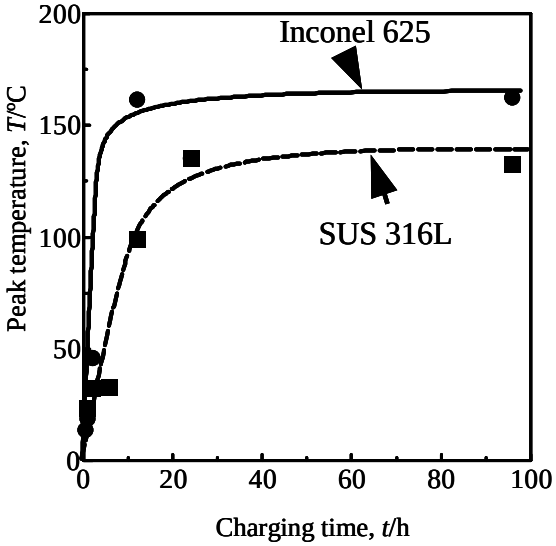

Fig. 2 The Relation between Charging Time and Peak Temperature for Inconel 625 and SUS 316L Charged by Electrolysis

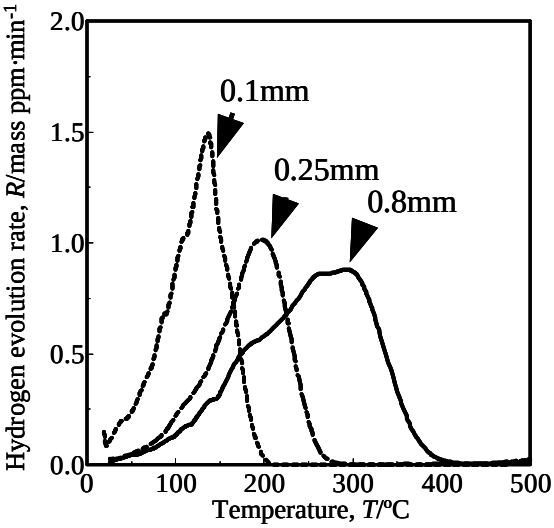

Fig. 4 Hydrogen Evolution Curves of Inconel 625 having Various Specimen Thicknesses when Hydrogen is Charged until Saturation by Electrolysis

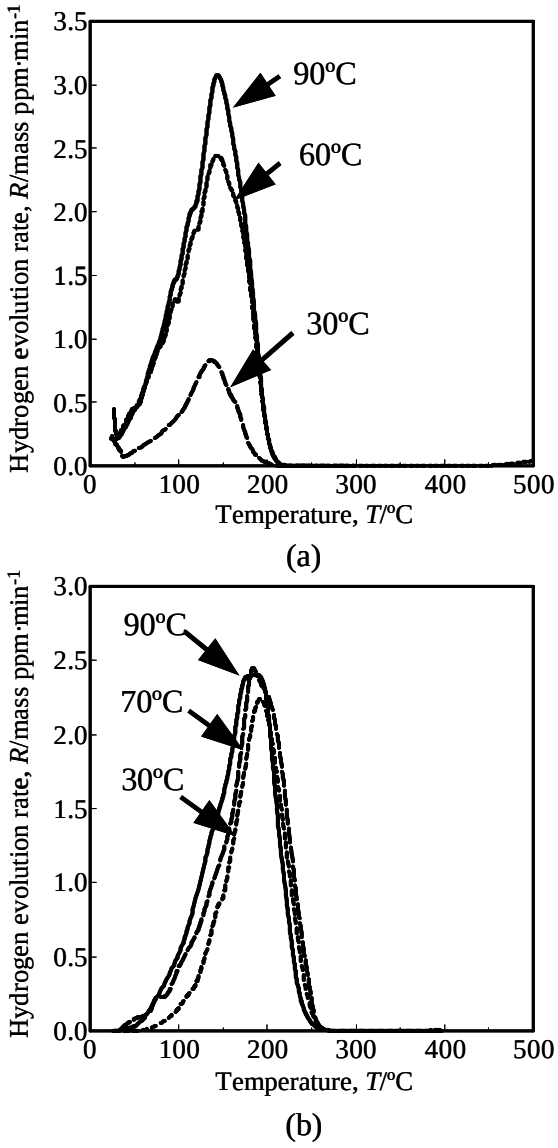

Fig. 5 Hydrogen Evolution Curves of (a) Inconel 625 and (b) SUS 316L respectively under Various Charging Temperatures when Hydrogen is Charged until Saturation by Electrolysis

case of hydrogen being charged until saturation. The peak temperatures and profiles of hydrogen desorption do not change with charging temperature. This suggests that the hydrogen states in the specimens do not change with charging temperature. The hydrogen contents in Inconel 625 and SUS 316L increase with charging temperature. The enthalpy of hydrogen solution is expressed as

$$\ln K_S = -\frac{\Delta S_S}{\mathrm{R}} + \frac{\Delta H_S}{\mathrm{R}T},$$

where K_S is the equilibrium factor , ΔS_S is the entropy of hydrogen solution, ΔH_S is the enthalpy of hydrogen solution and R is the gas constant. The ΔH_S values for Inconel 625 and SUS 316L are 17.4 and 6.9 kJ/mol, respectively. The values were employed when using Sieverts law.

3.2 Electrolysis and High-Pressure Charge

As shown earlier, the peak temperatures and profiles of hydrogen desorption depend on charging time and specimen thickness, but not on charging temperature. Fig. 6 (a) and (b) show hydrogen evolution curves of Inconel 625 and SUS 316L having a 0.1 mm specimen thickness when hydrogen was charged at 90 °C until saturation by electrolysis and high

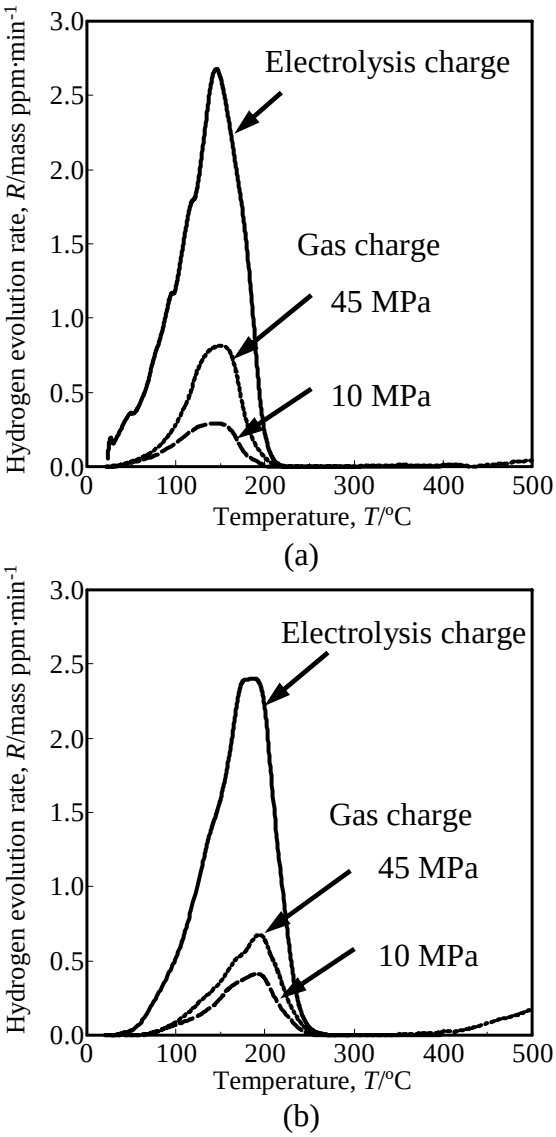

Fig. 6 Hydrogen Evolution Curves of (a) Inconel 625 and (b) SUS 316L having 0.1 mm of Specimen Thickness when Hydrogen is Charged at 90 °C until Saturation by Electrolysis and High Pressure.

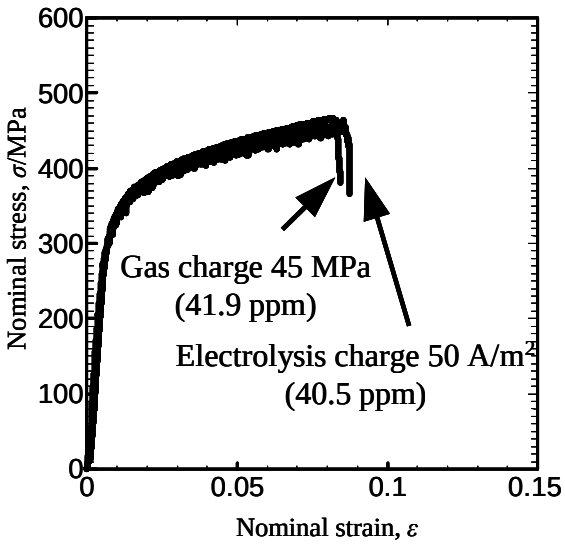

Fig. 7 Stress-Strain Curves of Inconel 625 when Strained in Air after Hydrogen is Charged until Saturation by Electrolysis and High-Pressure

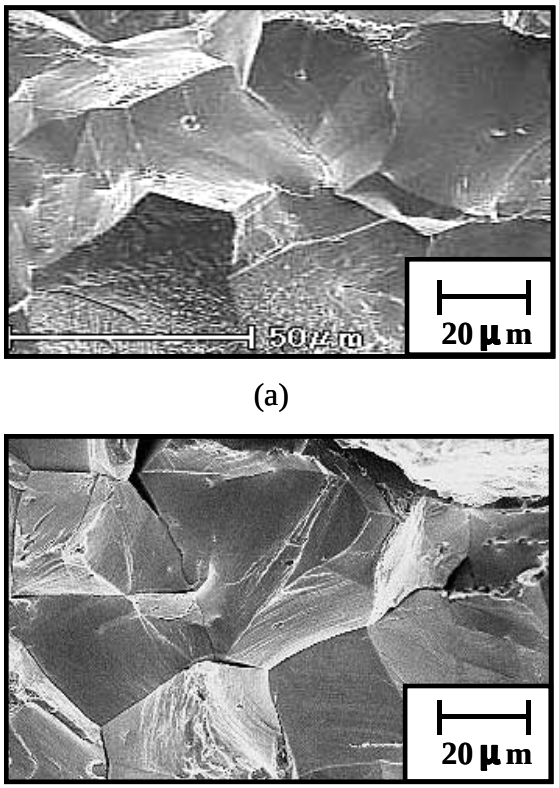

(a)

(b)

Fig. 8 SEM Images of Inconel 625 when Strained in Air after Hydrogen is Charged until Saturation by (a) Electrolysis (40.5 ppm) and (b) High Pressure (41.9 ppm)

pressure. The peak temperatures and profiles of hydrogen desorption from Inconel 625 and SUS 316L when hydrogen is charged by electrolysis are the same as those when hydrogen is charged by high pressure. Fig. 7 and 8 show the stress-strain curves and SEM images of Inconel 625, respectively, which was strained in air until fracture after hydrogen was charged by electrolysis and high pressure. The stress-strain curves and SEM images of Inconel 625 when hydrogen was charged by electrolysis are the same as those when hydrogen was charged by high pressure for similar hydrogen contents. These imply that hydrogen states after hydrogen charge by electrolysis are the same as those by high pressure. Furthermore, the hydrogen contents in the specimens when hydrogen is charged under extremely high fugacity exceed those under hydrogen pressure

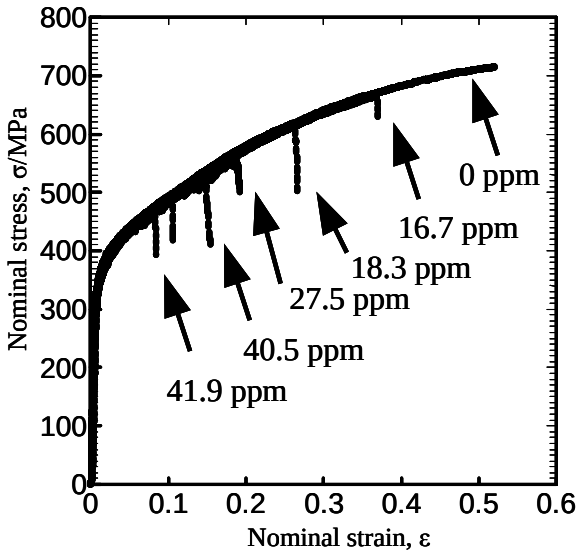

(a)

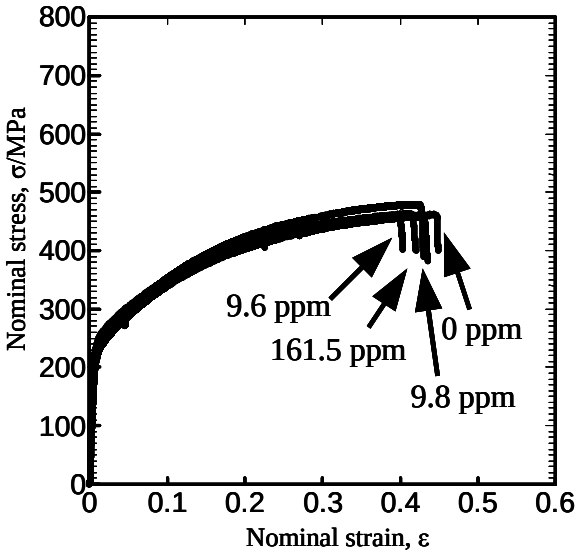

(b)

Fig. 9 Stress-Strain Curves of (a) Inconel 625 and (b) SUS 316L respectively when Strained in Air after Hydrogen is Charged by Electrolysis under Various Hydrogen Contents

of 45 MPa, as shown in Fig. 6. Thus, high-pressure gaseous charge can be substituted by electrolysis charge.

3.3 HYDROGEN EMBRITTLEMENT PROPERTIES

Many studies on hydrogen degradation of the austenitic stainless steels [3-5] have been conducted. In this study, the mechanical properties of Inconel 625 and SUS 316L absorbing various hydrogen contents were investigated. Fig. 9 (a) and (b) show the stress-strain curves of Inconel 625 and SUS 316L having a 0.25 mm and 0.2mm thickness respectively when they were strained in air after hydrogen was charged under various current densities. As hydrogen content increases, fracture strain in Inconel 625 decreases without changing yield strength and strain hardening rate. In contrast, fracture strain in SUS 316L does not change even when hydrogen content is 161.5 mass ppm. These show that susceptibility to hydrogen degradation is much lower in SUS 316L than in Inconel 625. Fig. 10 and 11 show the SEM images of fracture surfaces of Inconel 625 and SUS 316L, respectively, under various hydrogen contents. Without hydrogen, a dimple fracture surface is observed for Inconel 625. As hydrogen content increases, the fracture surface changes and looks brittle. In contrast, the fracture surfaces of

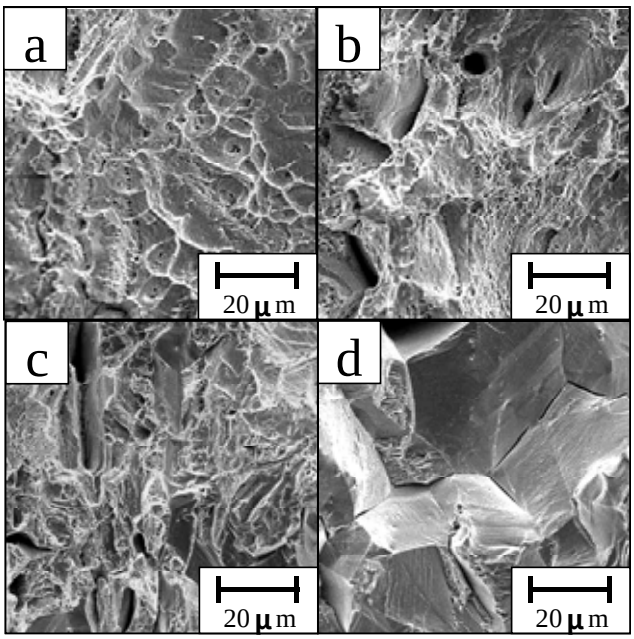

Fig. 10 SEM Images of the Fracture Surfaces of Inconel 625 when Hydrogen Content is (a) 0 ppm, (b) 16.7 ppm, (c) 27.5ppm and (d) 40.5 ppm.

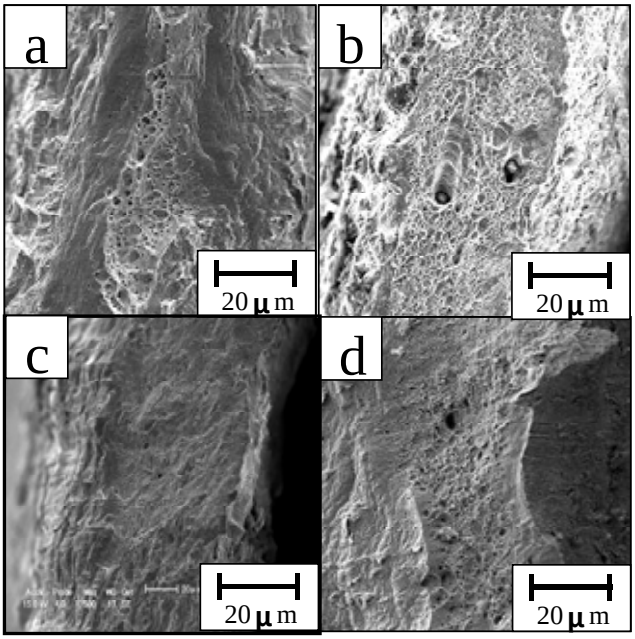

Fig. 11 SEM Images of the Fracture Surfaces of SUS 316L when Hydrogen Content is (a) 0 ppm, (b) 9.8 ppm, (c) 11.4 ppm and (d) 161.5 ppm.

SUS 316L are ductile dimples and do not change with hydrogen content. These degradation properties of Inconel 625 and SUS 316L with a thickness of 0.25 mm and 0.2 mm, respectively, are similar to the properties of the specimens with a thickness of 1.0 mm, though the results are omitted in this paper.

4 DISCUSSION

4.1 Transformation Using Sieverts Law

The hydrogen fugacity of electrolysis can be transformed into hydrogen pressure using Sieverts law and high-pressure gaseous charge is substituted by electrolysis charge. Sieverts law is expressed as

$$C = \mathrm{a}P^{1/2}\exp\left(-\frac{\Delta H_s}{\mathrm{R}T}\right),$$

where C is the hydrogen content, a is the constant factor, P is the hydrogen pressure and ΔH_S is the enthalpy of hydrogen solution. Fig. 12 shows the relationship between hydrogen gaseous pressure and hydrogen content in the case of gaseous hydrogen being charged at 90 °C. Hydrogen content increases with hydrogen pressure. Fig. 13 shows the

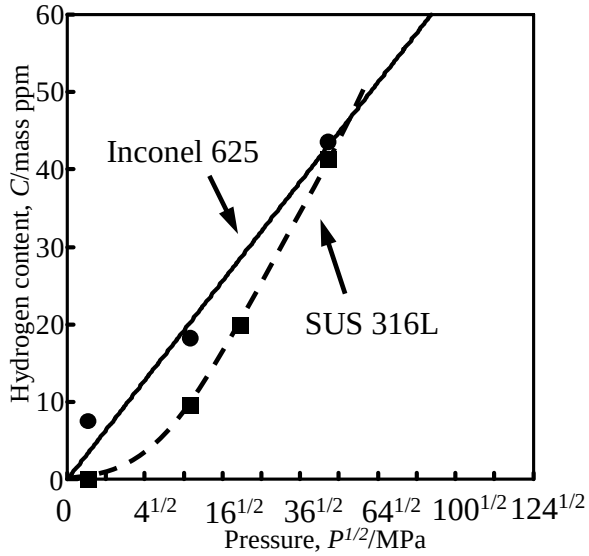

Fig. 12 The Relation between Hydrogen Gaseous Pressure and Hydrogen Content for Inconel 625 and SUS 316L when Gaseous Hydrogen is Charged at 90 °C until Saturation.

relationship between current density and hydrogen content. Hydrogen content increases with current density. Below 50 A/m^2, hydrogen is not absorbed in SUS 316L. This is due to the surface effects on the specimens. However, the effects are removed and sufficiently high hydrogen contents were achieved by adding NH_4SCN as a catalyst to electrolysis, though the results are omitted in this paper. The fugacities for the conditions of current density and NH_4SCN content that are required to absorb different hydrogen contents were transformed into hydrogen pressures at room temperature

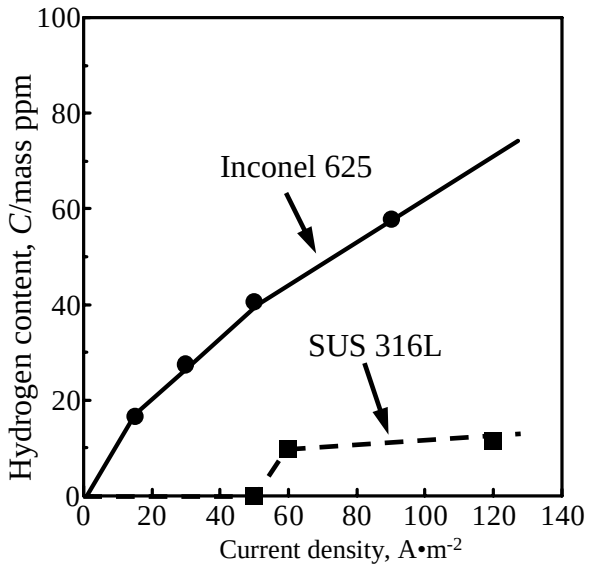

Fig. 13 The Relation between Current Density and Hydrogen Content for Inconel 625 and SUS 316L when Hydrogen is Charged by Electrolysis.

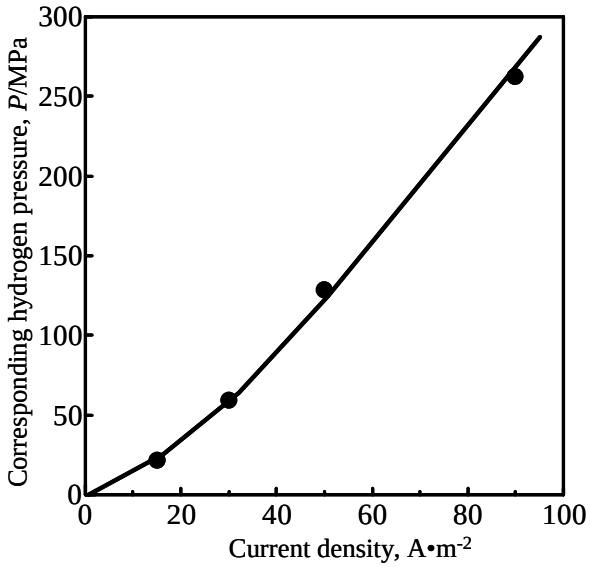

Fig. 14 The Relation between Substituted Hydrogen Pressure and Current Density for Inconel 625 when Hydrogen is Charged by Electrolysis.

using Sieverts law. Fig. 14 shows the relationship between corresponding hydrogen pressure, which is transformed at room temperature, and current density for Inconel 625. The hydrogen pressure increases with current density. Hydrogen pressure at room temperature corresponding to 90 A/m^2 is 262.5 MPa. This exceeds 100 MPa, which is the gaseous pressure used in hydrogen refueling stations. This indicates that high-pressure hydrogen environments in pipes or other components at hydrogen refueling stations can be qualifiedly substituted by electrolysis charge.

4.2 Hydrogen Degradation Mechanism

The fracture strains and fracture surfaces of Inconel 625 when hydrogen is charged under various substituted-hydrogen pressures using Sieverts law are as follows; (a) 52 percent, dimple (0 MPa), (b) 37 percent, small dimple + secondary crack (21.8 MPa), (c) 20 percent, secondary crack + flat facet (59.2 MPa) and (d) 16 percent, flat facet + intergranular (128.4 MPa). Although the fracture strain decreases and the fracture surface changes into a brittle like surface with increasing hydrogen content, the ductile features such as slip lines and small dimples still remain. Birnbaum [6-10] suggested a hydrogen-enhanced localized plasticity (HELP) mechanism using in situ observations of dislocation motion and fractographies for various materials. The observations in this

study are similar to those of Birnbaum. As hydrogen content increases, the stress required for dislocation motion decreases and deformation is locally enhanced. Extremely small voids nucleate at the intersections of slip lines, cracks easily propagate through them and then fracture strain decreases. In contrast, the fracture strain does not change and the fracture surfaces of SUS 316L remain dimpled even when hydrogen is charged under 206.2 MPa of substituted pressure.

5 CONCLUSIONS

1. The peak temperatures of thermal desorption depend on hydrogen charging time and specimen thickness, but not on charging temperature. This implies that hydrogen states do not change with charging temperature.

2. The peak temperatures and profiles of thermal desorption, stress-strain curves and SEM images of Inconel 625 and SUS 316L when hydrogen is charged by electrolysis are the same as those when hydrogen is charged by high pressure. These imply that hydrogen states do not depend on hydrogen charging methods.

3. Using Sieverts law, hydrogen pressures in the range of 0 to 262.5 MPa can be transformed using electrolysis charge. This means that hydrogen gaseous environments at 100 MPa in hydrogen refueling stations can be substituted by electrolysis charge.

4. Inconel 625 markedly suffers from hydrogen embrittlement in a substituted hydrogen environment of 100 MPa, but SUS 316L does not.

6 ACKNOWLEDGEMENTS

This study was supported by Industrial Technology Research Grant Program in 2005 from New Energy and Industrial Technology Development Organization (NEDO) of Japan.

7 REFERENCES

[1] 2004, *"Hydrogen Society"*, Feram, **9**, pp. 2-6 (in Japanese)

[2] Ministry of Economy, Trade and Industry, Press Releases, 2002, "meeting of fuel cell project team", http://www.meti.go.jp/kohosys/press/002765/1/020527fcpt.pdf

[3] Han G., He J., Fukuyama S. and Yokogawa K., 1998, "*Effect of strain-induced martensite on hydrogen environment embrittlement of sensitized austenitic stainless steels at low temperatures*", Acta Metall., **46**, pp. 4559-4570

[4] Walter R. J. and Chandler W. T., 1971, "*Influence of hydrogen pressure and notch severity on hydrogen-environment embrittlement at ambient temperatures*", Mater. Sci. Engng, **8**, pp. 90-97

[5] Williams D. P. and Nelson H. G., 1970, "*Embrittlement of 4130 steel by low-pressure gaseous hydrogen*", Metall. Trans., **1**, pp. 63-68

[6] Birnbaum H. K. and Sofronis P., 1994, "*Hydrogen-enhanced localized plasticity –a mechanism for hydrogen-related fracture*", Mater. Sci. Engng, **A176**, pp. 191-202

[7] Abraham D. P. and Altstetter C. J., 1995, "*Hydrogen-Enhanced Localization of Plasticity in an Austenitic Stainless Steel*", Metallurgical and Materials Transactions A, **26A**, pp. 2859-2871

[8] Robertson I. M. and Birnbaum H. K., 1986, "*An HVEM study of hydrogen effects on the deformation and fracture of nickel*", Acta Metall., **34**, pp. 353-366

[9] Rozenak P., Robertson I. M. and Birnbaum H. K., 1990, *" HEVM studies of the effects of hydrogen on the deformation and fracture of AISI type 316 austenitic stainless steel*", Acta Metall., **38**, pp. 2031-2040

[10] Shih D., Robertson I. M. and Birnbaum H. K., 1988, "*Hydrogen embrittlement of α titanium: in situ TEM studies*", Acta Metall., **36**, pp. 111-124